Inverse design for the one-dimensional Burgers equation

Thibault Liard* Enrique Zuazua*†‡

Abstract

In this paper, we study the problem of inverse design for the one-dimensional Burgers equation. This problem consists in identifying the set of initial data evolving to a given target at a final time. Due to the time-irreversibility of the Burgers equation, some target functions are unattainable from solutions of this equation, making the inverse problem under consideration ill-posed. To get around this issue, we introduce an optimal control problem which consists in minimizing the difference between the predictions of the Burgers equation and the observations of the system at a final time in $L^2(\mathbb{R})$ norm. The two main contributions of this work are the following:

- We fully characterize the set of minimizers of the aforementioned optimal control problem.
- A wave-front tracking method is implemented to construct numerically all of them.

One of minimizers is the backward entropy solution, constructed using a backward-forward method.

Keywords: Inverse problems; Conservation Laws; Entropy solutions; Backward-Forward approach; Optimal Control Problem; Wave-front tracking algorithm.

AMS classification: 35L65, 35F20, 93B30, 35R30.

1 Introduction

1.1 Presentation of the Problem

Inverse problems consist in finding the origin of a physical phenomenon, governed for instance by partial differential equations (PDEs), from a set of observations at a given time. Inverse problems arise naturally in meteorology, oceanography or climatology [29, 40, 21, 39, 26, 5, 18] to improve the forecasts of a model. Identification of initial states from measurements [31] and finding optimal positions or shapes of sensors [36, 37, 38] also lead to the study of inverse problems.

*Chair of Computational Mathematics, Fundación Deusto Av. de las Universidades 24, 48007 Bilbao, Basque Country, Spain.

†Chair in Applied Analysis, Alexander von Humboldt-Professorship, Department of Mathematics Friedrich-Alexander-Universitat, Erlangen-Nurnberg, 91058 Erlangen, Germany.

‡Departamento de Matemáticas, Universidad Autónoma de Madrid, 28049 Madrid, Spain.

This project has received funding from the European Research Council (ERC) under the European Union's Horizon 2020 research and innovation programme (grant agreement NO. 694126-DyCon). This work was partially supported by the ELKARTEK project KK-2018/00083 ROAD2DC of the Basque Government, by the Grant MTM2017-92996-C2-1-R/2-R COSNET of MINECO (Spain), by the Air Force Office of Scientific Research (AFOSR) under Award NO. FA9550-18-1-0242, by the Alexander von Humboldt-Professorship program, by the European Union's Horizon 2020 research and the innovation programme under the Marie Sklodowska-Curie grant agreement NO. 765579-ConFlex and by the grant ICON-ANR-16-ACHN-0014 of the French ANR.

The time-irreversibility of certain PDEs makes some inverse problems ill-posed, for instance:

- In the case of parabolic PDEs, the high and instant regularization effect induces the non-existence of initial data for which the corresponding solution evolves to given not-necessary regular target functions, and causes numerical instabilities when solving the PDE backwards in time. In [31], the authors solve an inverse problem for the heat equation with applications in identification of pollution source problems. Note however that, when the target is attainable, the initial datum whose the corresponding trajectory evolves to this target, is unique as seen in [32].
- In the case of nonlinear hyperbolic PDEs, the backward uniqueness property fails due to the presence of discontinuities (so-called *shocks*), i.e multiple initial data may evolve to the same attainable target function.

Thus, inverse problems need to be carefully addressed, depending on each type of PDEs.

In this paper, we consider the one-dimensional scalar conservation laws

$$\begin{cases} \partial_t u(t,x) + \partial_x f(u(t,x)) = 0, \quad (t,x) \in \mathbb{R}^+ \times \mathbb{R}, \\ u(0,x) = u_0(x), \end{cases} \tag{1}$$

where u is the state, u_0 is the initial state and the flux function f is a strictly convex function. The study of (1) may be motivated by the minimization of the sonic boom effects generated by supersonic aircrafts which are modeled by an augmented Burgers equation [14, 3, 2]. Since f is a strictly convex function, we assume that $f(u) = \frac{u^2}{2}$, without loss of generality.

Let $T > 0$ a final time and u^T a target function. As (1) is time-irreversibility, some conditions on u^T need to be imposed for it to be attainable. This is shown in [15, Theorem 3.1, Corollary 3.2], [24, Corollary 1] or [22] where they prove that u^T is truly attainable in an exact manner by a solution of (1) if and only if u^T satisfies the one-sided Lipschitz condition [8, 23, 35, 20], i.e

$$\partial_x u^T \leq \frac{1}{T} \text{ in } \mathcal{D}'(\mathbb{R}). \tag{2}$$

Due to the property of non-backward uniqueness of (1), there may exist multiple initial data leading to the same attainable target u^T, as seen in Figure 1. In [24], the authors prove that the set of initial data evolving to an attainable target u^T is a convex set. Later on, the aforementioned set was fully characterized in [15, Theorem 4.1] using the classical Lax-Hopf formula [28, Theorem 2.1].

Since we want to take into account unattainable target functions, an optimal control problem is introduced to solve the inverse problem of (1):

$$\inf_{u_0 \in \mathcal{U}_{\text{ad}}^0} J_0(u_0) := \|u^T(\cdot) - u(T,\cdot)\|_{L^2(\mathbb{R})}, \tag{$\mathcal{O}_T$}$$

where u is a solution of (1) defined in Section 2.1 and $\mathcal{U}_{\text{ad}}^0$ is the class of admissible initial data defined in (3).

To solve the optimal control problem ($\mathcal{O}_T$), some difficulties arise from a theoretical and numerical point of view.

- Since the entropy solution u of (1) may contain shocks even if the initial datum is a smooth function, this generates important added difficulties that have been the object of intensive

study in the past, see [34, 33, 9, 10, 6, 7, 4] and the references therein. In [9, 10, 6, 7], the derivative of the cost function J_0 in $(\mathcal{O}_T)$ is regarded in a weak sense by requiring strong conditions on the set of initial data. This leads to require that entropy solutions of (1) have a finite number of non-interacting jumps.

- When J_0 is weakly differentiable, gradient descent methods have been implemented in [11, 12, 1] to solve numerically the optimal problem $(\mathcal{O}_T)$. In the cases where it was applied successfully, only one possible initial datum emerges, namely the backward entropy solution, see Remark 1. This is mainly due to the numerical viscosity that numerical schemes introduce to gain stability. To find some multiple minimizers, the authors in [24] use a filtering step in the backward adjoint solution.

In this article, we give a full characterization of the set of minimizers for the optimal problem $(\mathcal{O}_T)$ in two steps.

Step 1. We prove that the backward entropy solution, denoted by $S_T^-(u^T)$, is an optimal solution of $(\mathcal{O}_T)$ using a backward-forward method described in Section 2.1.

Step 2. We show that u_0 is a minimizer of $(\mathcal{O}_T)$ if and only if the weak-entropy solution of (1) with initial datum u_0 coincides, at time T, with the weak-entropy solution of (1) with initial datum $S_T^-(u^T)$ using variational methods.

Contrary to [11, 12, 1], entropy solutions of (1), generated by the class of initial data $\mathcal{U}_{\text{ad}}^0$ in $(\mathcal{O}_T)$, may have a countable number of interacting jumps. Moreover, a wave-front tracking method is implemented to construct numerically, not just the backward entropy solution $S_T^-(u^T)$, but the set of minimizers of $(\mathcal{O}_T)$. An illustration of these results is given in Figure 2.

The article is organized as follows. In section 2, we describe the backward-forward method by introducing the forward operator S_T^+ and the backward operator S_T^-. Then, we solve the optimal control problem $(\mathcal{O}_T)$ in Section 2.2. In section 3, we construct numerically the set of minimizers of $(\mathcal{O}_T)$. More precisely, Section 3.1 is devoted to the construction of forward entropy solutions using a wave-front algorithm. Section 3.2, Section 3.3 and Section 3.4 explain how we pick up a random numerical element among the class of mimimizers of $(\mathcal{O}_T)$. Finally, we prove Theorem 2.1 in Section 4.

1.2 Some related open problems

Let us address some related open questions and possible extensions of this work.

- It would be interesting to consider a convex-concave function as a flux function in (1) which is, for instance, a more realistic choice to describe the flow of pedestrian [16, 13]. The main difficulty comes from the existence of discontinuities (called non-classical shocks) violating standard admissibility entropy conditions such that the Oleinik inequality.

- We could also study a Burgers equation with source terms. In this case, some suitable conditions on source terms has to be determined to use the backward-froward method described in this paper. For instance, the backward operator $S_t^-(u^T)$ defined in Section 2.1 associated to
$$\begin{cases} \partial_t u(t,x) + \partial_x f(u(t,x)) = -u^3(t,x), & (t,x) \in \mathbb{R}^+ \times \mathbb{R}, \\ u(T,\cdot) = u^T(x), & x \in \mathbb{R}. \end{cases}$$
may blow up at time $t < T$.

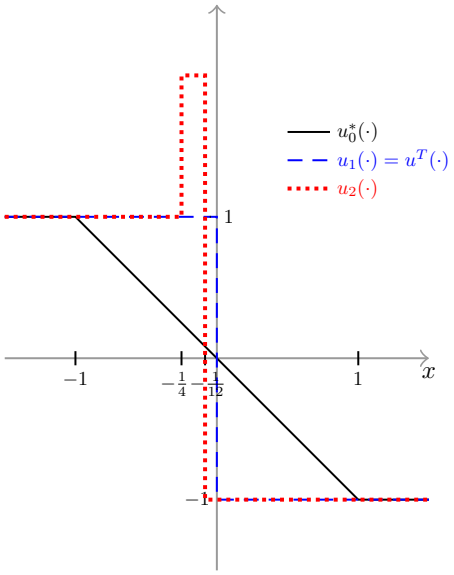

Figure 1: Three initial data $u_0^*(-)$, $u_1(--)$ and $u_2(\cdots)$ leading to a attainable target $u^T(\cdot) := \mathbb{1}_{(-\infty,0)}(\cdot) - \mathbb{1}_{(0,+\infty)}(\cdot)$ at time $T = 1$ along forward entropic evolution.

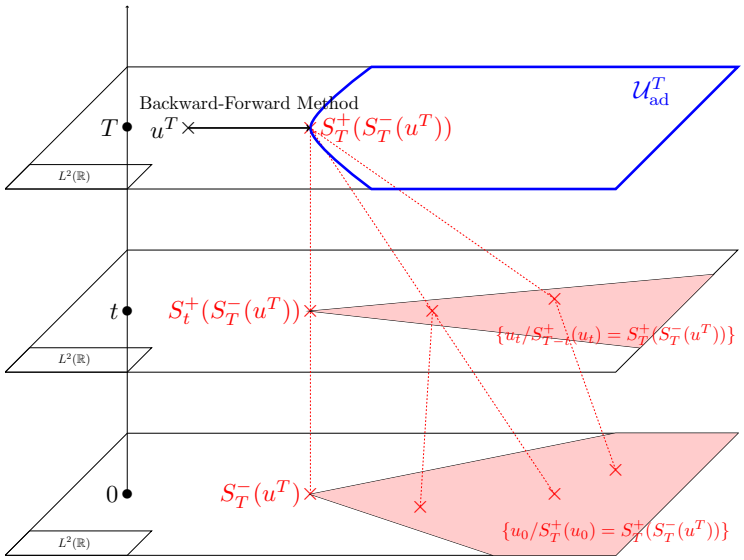

Figure 2: The backward-forward solution $S_T^+(S_T^-(u^T))$ is the projection of u^T onto the set of attainable target functions. The shaded area in red at time $t = 0$ represents the set of minimizers of $(\mathcal{O}_T)$.

- We can also investigate systems of conservation laws in one dimension (Euler equations, Saint-Venant equations, Aw-Rascle-Zhang traffic flow model). To apply the methods used in this paper, we need a full characterization of attainable targets and admissible initial data leading to a attainable target u^T at time T which is more difficult to obtain since the classical Lax-Hopf formula does not hold anymore. Note that, as soon as the backward-

forward operator $S_T^+(S_T^-)$ is well-defined, $S_T^+(S_T^-)(u^T)$ may give a good candidate to solve the inverse design of systems of conservation laws.

- We may consider a multi-dimensional equation of conservation of laws in a numerical point of view. For instance, a fractional steps method [17, 30, 25] (or splitting method) may be implemented to solve an inverse problem of a two-dimensional equation of conservation laws.

2 Main results and comments

2.1 The backward-forward method

For a sake of completeness, we recall the definition of a weak-entropy solution of (1).

Definition 2.1

- *We say that $u \in L^\infty(\mathbb{R}^+ \times \mathbb{R}) \cap C^0(\mathbb{R}^+, L^1_{loc}(\mathbb{R}))$ is a weak solution if for all $\varphi \in C^1_c(\mathbb{R}^2, \mathbb{R})$,*

$$\int_{\mathbb{R}^+}\int_{\mathbb{R}} (u\partial_t\varphi + f(u)\partial_x\varphi)dxdt + \int_{\mathbb{R}} u_0(x)\varphi(0,x)dx = 0.$$

- *We say that $u \in L^\infty(\mathbb{R}^+ \times \mathbb{R}) \cap C^0(\mathbb{R}^+, L^1_{loc}(\mathbb{R}))$ is a weak-entropy solution if u is a weak solution and for every $k \in \mathbb{R}$, for all $\varphi \in C^1_c(\mathbb{R}^2, \mathbb{R}^+)$,*

$$\int_{\mathbb{R}^+}\int_{\mathbb{R}} (|u-k|\partial_t\varphi + \mathrm{sgn}(u-k)(f(\rho)-f(k))\partial_x\varphi)dxdt + \int_{\mathbb{R}} |u_0-k|\varphi(0,x)dx \geq 0.$$

Kruzkov's theory [27] provides existence and uniqueness of a weak-entropy solution $(t,x) \to S_t^+(u_0)(x)$ of (1) with initial datum $u_0 \in L^\infty(\mathbb{R})$. For a given function u^T, we introduce the function $(t,x) \to S_t^-(u^T)(x)$ as follows: for every $t \in [0,T]$, for a.e $x \in \mathbb{R}$,

$$S_t^-(u^T)(x) = S_t^+(x \to u^T(-x))(-x).$$

Remark 1 *The solutions $S_t^+(u_0)$ and $S_t^-(u^T)$ may be regarded as the zero viscosity limit of the solutions $S_t^{+,\epsilon}(u_0)$ and $S_T^{-,\epsilon}(u^T)$ respectively where $S_t^{+,\epsilon}(u_0)$ and $S_t^{-,\epsilon}(u^T)$ are defined as follows: $S_t^{+,\epsilon}(u_0)$ is the solution of the following viscous Burgers equation*

$$\begin{cases} \partial_t u(t,x) + \partial_x f(u(t,x)) = +\epsilon\partial^2_{xx}u(t,x), & (t,x) \in \mathbb{R}^+ \times \mathbb{R}, \\ u(0,\cdot) = u_0(x), & x \in \mathbb{R}, \end{cases}$$

and $S_t^{-,\epsilon}(u_0)$ is the solution of the following backward equation

$$\begin{cases} \partial_t u(t,x) + \partial_x f(u(t,x)) = -\epsilon\partial^2_{xx}u(t,x), & (t,x) \in \mathbb{R}^+ \times \mathbb{R}, \\ u(T,\cdot) = u^T(x), & x \in \mathbb{R}. \end{cases}$$

Using the change of variable $(t,x) \to (T-t,-x)$, we notice that the backward equation above is well-defined. Thus, $S_T^-(u^T)$ is called the backward entropy solution.

The backward-forward method consists in solving backward in time the PDE (1) with final target u^T and then solving it forward in time with initial datum $S_T^-(u^T)$, the solution of the backward PDE.

For any attainable target u^T, we have $S_T^+(S_T^-(u^T)) = u^T$ as seen in [15, Theorem 3.1, Corollary 3.2] and [24, Corollary 1]. however, there exist some target functions u^T verifying $S_T^+(S_T^-(u^T)) \neq u^T$ as seen in Example 1.

Example 1 *Assuming that u^T is defined by $u^T(\cdot) = -\mathbb{1}_{(-\infty,0)}(\cdot)+\mathbb{1}_{(0,\infty)}(\cdot)$ then the weak-entropy solution v of (1) with initial datum $v(0,x) = u^T(-x)$ is defined by*

$$v(t,x) = \begin{cases} 1 & \text{if } x < 0, \\ -1 & \text{if } x > 0. \end{cases}$$

Thus, $S^-_{T-t}(u^T) : x \to v(T-t,-x)$ is a weak solution of (1) verifying that $u(T) = u^T$. The weak-entropy solution u_e with initial datum $v(T,-x)$ is defined by

$$u_e(t,x) = \begin{cases} -1 & \text{if } x < -t, \\ \frac{x}{t} & \text{if } -t \le x \le t, \\ 1 & \text{if } t < x. \end{cases}$$

In particular, $S^+_T(S^-_T(u^T)) := u_e(T) \neq u^T$. Note that u^T is an unattainable target.

2.2 An optimal problem

We denote by $BV(\mathbb{R})$ and $SBV(\mathbb{R})$, the class of functions of bounded variation and the class of special bounded variation respectively. Both sets are defined for instance in [20, Definition 1.7.1] and [20, Definition 1.7.9] respectively. From now on, we assume that $K^T \subset \mathbb{R}$ is an open bounded interval such that $\text{supp}(u^T) \subset K^T$ and the class of admissible initial data $\mathcal{U}^0_{\text{ad}}$ in $(\mathcal{O}_T)$ is defined by

$$\mathcal{U}^0_{\text{ad}} = \{u_0 \in BV(\mathbb{R}) / \|u_0\|_{BV(\mathbb{R})} < C \text{ and } \text{supp}(u_0) \subset K_0\}. \tag{3}$$

where $C > 0$ is a constant such that $\|S^-_T(u^T)\|_{BV(\mathbb{R})} < C$. Above, supp stands for the support of the function u^T. Theorem 2.1 characterizes the set of optimal solutions for $(\mathcal{O}_T)$.

Theorem 2.1 *Let $u^T \in BV(\mathbb{R})$. The optimal control problem $(\mathcal{O}_T)$ admits multiple optimal solutions. Moreover, for a.e $T > 0$, the initial datum $u_0 \in BV(\mathbb{R})$ is an optimal solution of $(\mathcal{O}_T)$ if and only if $u_0 \in BV(\mathbb{R})$ verifies $S^+_T(u_0) = S^+_T(S^-_T(u^T))$.*

In the sequel, we use the notation $g(x-) := \lim_{\substack{y \to x \\ y<x}} g(y)$ and $g(x+) := \lim_{\substack{y \to x \\ x<y}} g(y)$. Note that both limits exist if $g \in BV(\mathbb{R})$. Corollary is a direct consequence of Theorem 2.1 and the full characterization of the set $\{u_0 \in BV(\mathbb{R}) / S^-_T(u_0) = S^-_T(u^T)\}$ given in Theorem A.2.

Corollary 2.1 *We denote by $(x^T_i)_{i\in\{1,\cdots,N\}}$ the $N \in \mathbb{N}\cup\{\infty\}$ discontinuous points of $S^+_T(S^-_T(u^T))$ such that $S^+_T(S^-_T(u^T))(x^T_i+) < S^+_T(S^-_T(u^T))(x^T_i-)$. Let*

$$\underline{a}_i := x^T_i - Tf'(S^+_T(S^-_T(u^T))(x^T_i-)) \quad \text{and} \quad \overline{a}_i := x^T_i - Tf'(S^+_T(S^-_T(u^T))(x^T_i+)).$$

For a.e $T > 0$, $u_0 \in BV(\mathbb{R})$ is an optimal solution of $(\mathcal{O}_T)$ if and only if the two following statements hold:

- *For every $x \in \mathbb{R}\setminus \cup_{i=1}^N [\underline{a}_i, \overline{a}_i]$, $u_0(x-) = S^-_T(u^T)(x-)$.*
- *For every $x \in \cup_{i=1}^N [\underline{a}_i, \overline{a}_i]$,*

$$\int_{\underline{a}_i}^{x} u_0(s)\,ds \ge \int_{\underline{a}_i}^{x} S^-_T(u^T)(s)\,ds,$$
$$\int_{\underline{a}_i}^{\overline{a}_i} u_0(s)\,ds = \int_{\underline{a}_i}^{\overline{a}_i} S^-_T(u^T)(s)\,ds.$$

Remark 2

- *Since $u^T \in BV(\mathbb{R})$ and $u_0 \in BV(\mathbb{R})$, a wave-front tracking algorithm, described in Section 3, can be implemented to construct the set of minimizers of $(\mathcal{O}_T)$. Note that, from [20, Theorem 11.2.2], weak-entropy solutions of (1), with initial data in $L^\infty(\mathbb{R})$, belong to the set of $BV_{loc}(\mathbb{R})$ functions.*

- *The assumption "for a.e $T > 0$" in Theorem 2.1 and Corollary 2.1 can be replaced by the condition "for every $T > 0$ verifying that $S_T^-(u^T) \in SBV(\mathbb{R})$ and $S_T^+(S_T^-(u^T)) \in SBV(\mathbb{R})$". This is due to [20, Theorem 11.3.5] which states that, for any $u_0 \in L^\infty(R)$, for a.e $t \in (0, +\infty)$, $S_t^+(u_0)$ belongs to the set of $SBV_{loc}(\mathbb{R})$ function. Note that, $S_T^+(S_T^-(u^T)) \in SBV(\mathbb{R})$ and $S_T^-(u^T) \in SBV(\mathbb{R})$ are necessary conditions to apply Theorem A.1 and Theorem A.2.*

Remark 3

- *The constraints $\|u_0\|_{BV(\mathbb{R})} \leq C$ and $Supp(u_0) \subset K_0$ are used to guarantee the existence of optimal solutions of $(\mathcal{O}_T)$. More precisely, the constraint $Supp(u_0) \subset K_0$ leads to $Supp(S_T^+(u_0)) \subset \tilde{K}$ where $\tilde{K}$ is also an open bounded interval using the finite velocity of propagation of Burgers equation and the forward maximum principle, see Lemma 4.1. Moreover, the minimizing sequence $(u_0^n)_{n\in\mathbb{N}}$ of $(\mathcal{O}_T)$ satisfies $\|u_0^n\|_{BV(\mathbb{R})} \leq C$. Therefore, we can apply Helly's Theorem which states the compactness of the embedding $BV_{loc}(\mathbb{R}) \subset L^2_{loc}(\mathbb{R})$. Note that, since $\|S_T^-(u^T)\|_{BV(\mathbb{R})} < C$, we have $\|S_T^+(S_T^-(u^T))\|_{BV(\mathbb{R})} < C$ and so the constraint is inactive.*

The proof of Theorem 2.1 is structured as follows. From [15, Theorem 3.1, Corollary 3.2], [24, Corollary 1] or [22], there exists $u_0 \in BV(\mathbb{R})$ such that $S_T^+(u_0) = q$ if and only if q satisfies the one-sided Lipschitz condition (2). Thus, the optimal problem $(\mathcal{O}_T)$ can be rewritten as follows.

$$\min_{q\in\mathcal{U}_{\rm ad}^T} J_1(q) := \|u^T - q\|_{L^2(\mathbb{R})}, \tag{4}$$

where the admissible set $\mathcal{U}_{\rm ad}^T$ is defined by

$$\mathcal{U}_{\rm ad}^T = \{q \in BV(\mathbb{R})/\ \partial_x q \leq \frac{1}{T} \text{ and } \|q\|_{BV(\mathbb{R})} \leq C \text{ and } \mathrm{Supp}(q) \subset K_1\}.$$

Above, K_1 an open bounded interval such that $\tilde{K} \subset K_1$ with $\tilde{K}$ an open bounded interval defined in Lemma 4.1. Note that the optimal problem (4) is not related to the PDE model (1). We prove that $q = S_T^+(S_T^-(u^T))$ is a critical point of (4) using the first-order optimality conditions applied to (4) and the full characterization of the set $\{u_0 \in BV(\mathbb{R})/S_T^-(u_0) = S_T^-(u^T)\}$ given in Theorem A.2.

3 Applications and numerical investigations

Fix $a, b, \underline{u}, \overline{u} \in \mathbb{R}$ such that $a < b$ and $\underline{u} < \overline{u}$. We consider the set of initial data $u_0 \in BV(\mathbb{R})$ such that, for every $x \in (-\infty, a)$, $u_0(x) = u_0(a-) \in [\underline{u}, \overline{u}]$, for every $x \in (b, \infty)$, $u_0(x) = u_0(b+) \in [\underline{u}, \overline{u}]$ and for every $x \in \mathbb{R}$, $\underline{u} \leq u_0(x) \leq \overline{u}$.

3.1 Wave-front tracking algorithm

To solve (1) with initial datum $u_0 \in BV(\mathbb{R})$, we use a wave-front tracking algorithm proposed by Dafermos [19]. Since our aim is to track in time the discontinuity of the solution u of (1) with initial datum u_0, we pay special attention to the discontinuity of u_0 in the construction of the state mesh $\mathcal{M}_n$. More precisely, we denote by $(x_0^i)_{1\leq i\leq N}$, the $N \in \mathbb{N}$ discontinuous points of u_0 and we construct a state mesh $\mathcal{M}_n := \{u_j^n\}_{j=0}^{M_n}$ sorted in ascending order such that $u_0^n = \underline{u}$, $u_{M_n}^n = \overline{u}$

and for every $i \in \{1, \cdots, N\}$, $u_0(x_0^i-), u_0(x_0^i+) \in \mathcal{M}_n$. We construct an approximate piecewise constant function $u_0^n : \mathbb{R} \to \mathcal{M}_n$ of u_0 such that, for every $1 \leq i \leq N$, $u_0^n(x_0^i-) = u_0(x_0^i-) \in \mathcal{M}_n$ and $u_0^n(x_0^i+) = u_0(x_0^i+) \in \mathcal{M}_n$. In the sequel, we denote by $(x_0^{i,n})_{i=1,\cdots,N_n}$ with $N_n \geq N$ the discontinuous points of u_0^n.

- If $u_0^n(x_0^{i,n}-) > u_0^n(x_0^{i,n}+)$, a shock wave $(u_0^n(x_0^{i,n}-), u_0^n(x_0^{i,n}+))$ is created with speed given by the Rankine-Hugoniot condition.
- If $u_0^n(x_0^{i,n}-) < u_0^n(x_0^{i,n}+)$, we split the rarefaction wave $(u_0^n(x_0^{i,n}-), u_0^n(x_0^{i,n}+))$ into a fan of rarefaction shocks; since, for a.e $x \in \mathbb{R}$, $u_0^n(x) \in \mathcal{M}_n$, there exists $j_0 < j_1$ such that $u_0^n(x_0^{i,n}-) = u_{j_1}^n$ and $u_0^n(x_0^{i,n}+) = \rho_{j_0}^n$. We create $j_1 - j_0$ rarefaction shocks $(u_j^n, u_{j+1}^n)_{j=j_0,\cdots,j_1-1}$ with speed prescribed by the Rankine-Hugoniot condition.

Thus, solving approximately the Riemann problem at each point of discontinuity of u_0^n as described above and piecing solutions together, we construct a solution u^n until two waves meet at time t_1. The approximate solution $u^n(t_1, \cdot)$ is a piecewise constant function verifying $u^n(t_1, x) \in \mathcal{M}_n$ for a.e $x \in \mathbb{R}$, the corresponding Riemann problems can again be approximately solved within the class of piecewise constant functions and so on.

In the sequel, we denote by $S_t^{+,n}(u_0)$, the approximate solution of (1) with initial datum u_0 at time t constructed using the wave-front tracking algorithm.

Example 2 *We assume that u_0 is a N-wave defined by*

$$u_0(x) = \begin{cases} 0, & \text{if } x < 0, \\ -1 + 2x, & \text{if } 0 < x < 1, \\ 0, & \text{if } 1 < x. \end{cases}$$

In this case, $a = 0$, $b = 1$, $\underline{u} = -1$ and $\overline{u} = 2$. The state mesh $\mathcal{M}_n$ is defined by

$$\mathcal{M}_n := -1 + 3(2^{-n}\mathbb{N} \cap [0, 1]),$$

with $n = 5$. The discontinuous points of u_0 are located at $x = 0$ and $x = 1$ with $u_0(0-) = 0 \in \mathcal{M}_n$, $u_0(0+) = -1 \in \mathcal{M}_n$, $u_0(1-) = 1 \in \mathcal{M}_n$, and $u_0(1+) = 0 \in \mathcal{M}_n$. In Figure 3, an approximate function $u_0^n : \mathbb{R} \to \mathcal{M}_n$ of u_0 is constructed. In Figure 5, the values of $S_T^{+,n}(u_0^n)$ at time $T = 1$ and $T = 2$ are extracted from Figure 4.

3.2 A geometrical interpretation of Theorem A.1

Let $u_L > u_R$, $\bar{x} \in \mathbb{R}$ and $T > 0$, we introduce the set

$$\Gamma(u_L, u_R, \bar{x}, T) := \left\{\gamma \in W^{1,1}\left([\bar{x} - Tf'(u_L), \bar{x} - Tf'(u_R)], \mathbb{R}\right) / \dot{\gamma} \in BV(\mathbb{R})\right\}$$

defined by $\gamma \in \Gamma(u_L, u_R, \bar{x}, T)$ if

(A1) $\gamma(\bar{x} - Tf'(u_L)) = 0$,

(A2) $\gamma(\bar{x} - Tf'(u_R)) = T(u_L f'(u_L) - f(u_L) - u_R f'(u_R) + f(u_R))$,

(A3) for every $x \in [\bar{x} - Tf'(u_L), \bar{x} - Tf'(u_R)]$,

$$\gamma(x) \geq \gamma_*(x) := -T \int_{u_L}^{(f')^{-1}(\frac{\bar{x}-x}{T})} sf''(s)ds.$$

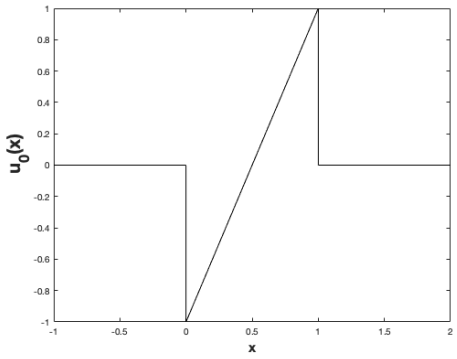

Initial datum u_0

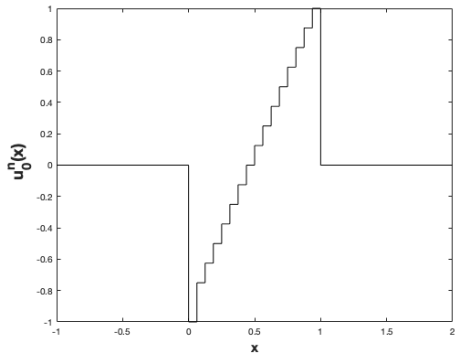

Approximate initial datum u_0^n with $n = 5$

Figure 3: Construction of an approximate initial datum $u_0^n : x \to \mathcal{M}_n$ of u_0 with $n = 5$.

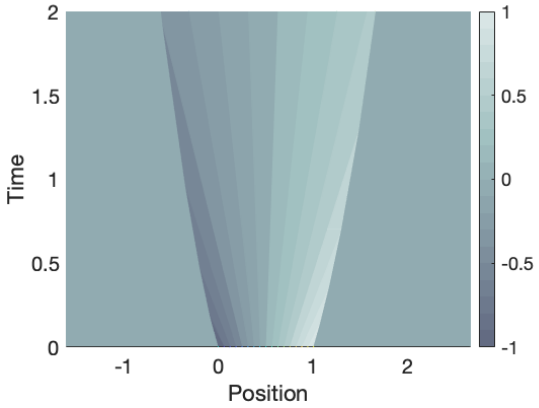

Figure 4: Plotting of $(t, x) \to S_t(u_0)(t, x)$ with u_0 defined in Example 2

For a.e $x \in [\bar{x} - Tf'(u_L), \bar{x} - Tf'(u_R)]$, $\dot{\gamma}_*(x) = S_T^+(S_T^-(u^T))(x)$. An illustration of the set $\Gamma(u_L, u_R, \bar{x}, T)$ is given in Figure 6. Theorem A.1 can be written as follows:

Corollary 3.1 *Assuming that $u^T \in SBV(\mathbb{R})$ is a attainable target and we denote by $(x_i^T)_{i=\{1,\cdots,N\}}$ the discontinuous points of u^T with $N \in \mathbb{N} \cup \{\infty\}$. The initial datum $u_0 \in BV(\mathbb{R})$ satisfies $S_T^+(u_0) = u^T$ if and only if the two following statements hold*

- *$u_0(x-) = S_T^-(u^T)(x-)$ for every $x \in \mathbb{R} \setminus \cup_{i=1}^N [x_i^T - Tf'(u^T(x_i^T-)), x_i^T - Tf'(u^T(x_i^T+))]$.*
- *For every $i \in \{1, \cdots, N\}$, there exists $\gamma_i \in \Gamma(u^T(x_i^T-), u^T(x_i^T+), x_i^T, T)$ such that $u_0(x) = \dot{\gamma}_i(x)$ for almost every $x \in [x_i^T - Tf'(u^T(x_i^T-)), x_i^T - Tf'(u^T(x_i^T+))]$.*

Thus, u_0 is uniquely determined by u^T and $\cup_{i=1}^N \gamma_i$ which is denoted afterward by $u_0 \equiv [u^T; \cup_{i=1}^N \gamma_i]$.

Corollary 3.1 points out the richness and the diversity of initial data evolving to the same target at time T.

- There exists $u_0 \in BV(\mathbb{R})$ such that $S_T^+(u_0) = u^T$ with $\min_{x\in\mathbb{R}} u_0(x) < \min_{x\in\mathbb{R}} u^T(x)$ and/or $\max_{x\in\mathbb{R}} u^T(x) < \max_{x\in\mathbb{R}} u_0(x)$, see Figure 10.

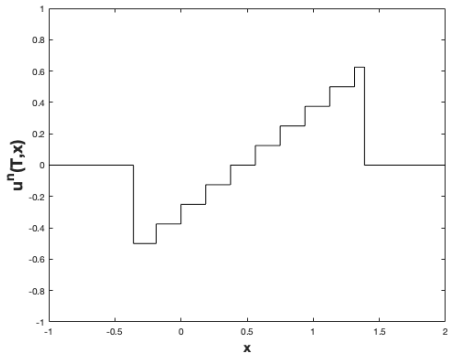

Approximate solution $S_T^{+,n}(u_0^n)$ at $T = 1$.

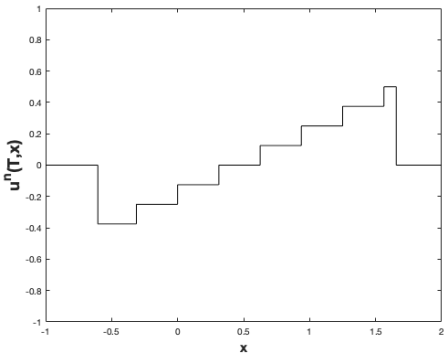

Approximate solution $S_T^{+,n}(u_0^n)$ at $T = 2$.

Figure 5: Construction of an approximate solution $u^n(T,\cdot) := S_T^{+,n}(u_0^n)$ of (1) using a wave-front algorithm with discretization parameter $n = 5$.

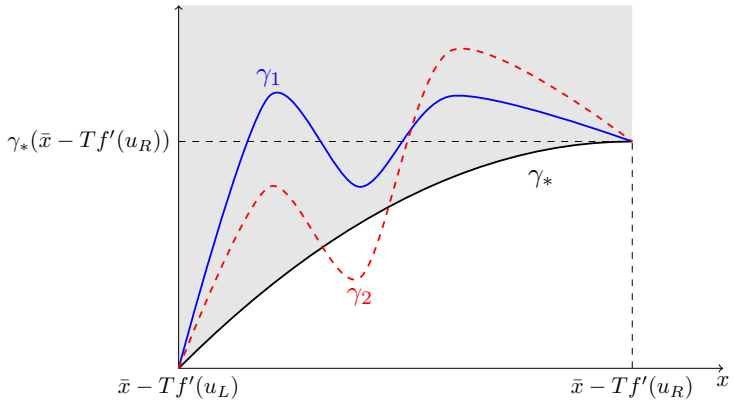

Figure 6: The set $\Gamma(u_L, u_R, \bar{x}, T)$ is illustrated by the shaded area. The function γ_* is defined by $\gamma_*(x) = -T\int_{u_L}^{(f')^{-1}(\frac{\bar{x}-x}{T})} sf''(s)ds$ with $x \in [\bar{x} - Tf'(u_L), \bar{x} - Tf'(u_R)]$. We have $\dot{\gamma}_* = S_T^+(S_T^-(u^T))$, $\gamma_1 \in \Gamma(u_L, u_R, \bar{x}, T)$ and $\gamma_2 \notin \Gamma(u_L, u_R, \bar{x}, T)$.

- The set $\{u_0 \in BV(\mathbb{R})/S_T^+(u_0) = u^T\}$ is a convex cone having as unique extremal point at its vertex the map $S_T^-(u^T)$, see [15, Proposition 5.2]. If $u_0 \equiv [u^T; \gamma]$ with $\gamma \in \Gamma(u_L, u_R, \bar{x}, T)$ and $u_0^* \equiv [u^T; \gamma_*]$ with γ_* defined in **(A3)** then, from Figure 6, we immediately see that $\gamma_* + \eta(\gamma - \gamma_*) \in \Gamma(u_L, u_R, \bar{x}, T)$. Therefore for every $\eta > 0$, $u_0^\eta \equiv [u^T, \gamma_* + \eta(\gamma - \gamma_*)]$ satisfies $S_T^+(u_0^\eta) = u^T$. Thus, we have $u_0^\eta = u_0^* + \eta(u_0 - u_0^*)$.

Example 3 shows that the three initial data u_0^*, u_1 and u_2 defined in Figure 1 verifies $S_T^+(u_0^*) = S_T^+(u_1) = S_T^+(u_2) = u^T$ using Corollary 3.1.

Example 3 *We consider the target function* $u^T(\cdot) := \mathbb{1}_{(-\infty,0)}(\cdot) - \mathbb{1}_{(0,+\infty)}(\cdot)$ *and we construct three different initial data defined by, for a.e* $x \in \mathbb{R}$, $u_0^*(x) = \mathbb{1}_{(-\infty,-1)}(x) - x\mathbb{1}_{(-1,1)}(x) - \mathbb{1}_{(1,+\infty)}(x)$, $u_1(x) = \mathbb{1}_{(-\infty,0)}(x) - \mathbb{1}_{(0,+\infty)}(x)$ *and* $u_2(x) = \mathbb{1}_{(-\infty,-\frac{1}{4})}(x) + 2\mathbb{1}_{(-\frac{1}{4},-\frac{1}{12})}(x) - \mathbb{1}_{(-\frac{1}{12},+\infty)}(x)$, *see Figure 1. Let* $\gamma_* : [-1,1] \to \mathbb{R}$, $\gamma_1 : [-1,1] \to \mathbb{R}$ *and* $\gamma_2 : [-1,1] \to \mathbb{R}$ *be three functions such that, for a.e* $x \in [-1,1]$, $\dot{\gamma}_*(x) = u_0^*(x)$, $\dot{\gamma}_1(x) = u_1(x)$ *and* $\dot{\gamma}_1(x) = u_1(x)$ *then we immediately see*

that γ_*, γ_1 and γ_2 belongs to $\Gamma(1,-1,0,1)$, see Figure 7. Thus, from Corollary 3.1, u_0^*, u_1 and u_2 verifies $S_T^+(u_0^*) = S_T^+(u_1) = S_T^+(u_2) = u^T$.

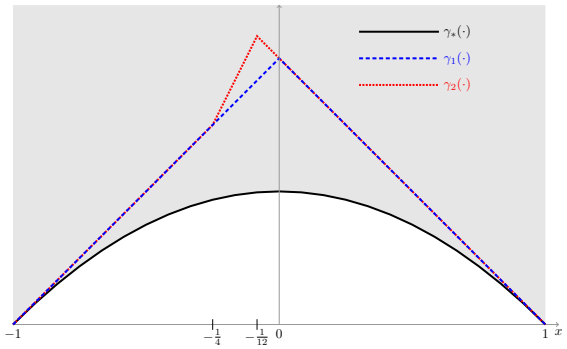

Figure 7: Plotting of γ_*, γ_1 and γ_2 belonging to $\Gamma(1,-1,0,1)$. For a.e $x \in [-1,1]$, $\dot{\gamma}_*(x) = u_0^*(x)$, $\dot{\gamma}_1(x) = u_1(x)$ and $\dot{\gamma}_2(x) = u_2(x)$ where u_0^*, u_1 and u_2 are defined in Figure 1.

The proof of Corollary 3.1 is an immediate consequence of Theorem A.1 using $\gamma_i(x) = \int_{\underline{a}_i}^x u_0(s)ds$ and $\gamma_*(x) = \int_{\underline{a}_i}^x S_T^-(u^T)(s)ds$.

Remark 4 *The characterization given in Corollary 3.1 may be easily adapted to the case where some constraints are added on the state u. If there exist $\underline{u}$ and $\bar{u}$ such that $\underline{u} \leq S_t^+(u_0) \leq \bar{u}$ for every $t \in [0,T]$ then Corollary 3.1 holds if we require that $\gamma \in \Gamma(u_L, u_R, \bar{x}, T)$ also satisfies the constraint $\dot{\gamma}(x) \in [\underline{u}, \bar{u}]$ for almost every $x \in [\bar{x} - Tf'(u_L), \bar{x} - Tf'(u_R)]$.*

3.3 Construction of the set of admissible initial data using Wave-front tracking algorithm

We assume that $u^T = u_L \mathbb{1}_{(-\infty,\bar{x})} + u_R \mathbb{1}_{(\bar{x},\infty)}$ with $u_L > u_R$. As explained in Section 3.1, the constructed state mesh $\mathcal{M}_n := \{u_i^n\}_{i=0}^N$ includes u_L and u_R. Our aim is to construct randomly the set of initial data $u_0^n \in \mathcal{M}_n$ such that $S_T^{+,n}(u_0^n) = u^T$. To that end, we introduce the set $\Gamma^n(u_L, u_R, \bar{x}, T)$ defined by

$$\Gamma^n(u_L, u_R, \bar{x}, T) = \{\gamma^n \in \Gamma(u_L, u_R, \bar{x}, T) / \dot{\gamma}^n(x) \in \mathcal{M}_n, \text{ for a.e } x \in [\bar{x} - Tf'(u_L), \bar{x} - Tf'(u_R)]\}$$

In particular, we have $\underline{u} := u_0^n \leq \dot{\gamma}^n(x) \leq u_{M_n}^n := \overline{u}$. Let $M \in \mathbb{N}$, we construct the set of piecewise constant functions $\gamma^n \in \Gamma^n(u_L, u_R, \bar{x}, T)$ admitting $M \in \mathbb{N}$ discontinuous points $(X_i, Y_i)_{i\in\{1,\cdots,M\}}$ via the following random iterative procedure (see Figure 8).

The iterative construction is initiated with $(X_1, Y_1) = (\bar{x} - Tf'(u_L), 0)$. Then, we construct $(X_i, Y_i)_{i\in\{1,\cdots,M\}}$ such that, for every $i \in \{2, \cdots, M\}$,

$$\gamma_*(X_i) \leq Y_i \leq \min(u_0^n(X_i - \bar{x} + Tf'(u_L)), u_n^{M_n}(X_i - \bar{x} + Tf'(u_R)) + \gamma_*(\bar{x} - Tf'(u_R))), \tag{5}$$

and, for every $i \in \{1, \cdots, M\}$,

$$\frac{Y_{i+1} - Y_i}{X_{i+1} - X_i} \in \mathcal{M}_n, \tag{6}$$

with $(X_{M+1}, Y_{M+1}) := (\bar{x} - Tf'(u_R), \gamma^*(\bar{x} - Tf'(u_R)))$. From a point (X_i, Y_i) with $i \in \{1, \cdot, M-1\}$, there exists a discrete set of (X_{i+1}, Y_{i+1}) such that (5) and (6) hold as seen in Figure 8 by red

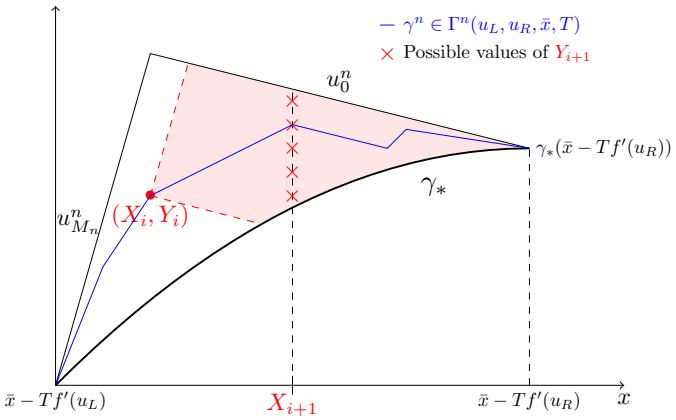

Figure 8: Construction of a random piecewise constant $\gamma^n \in \Gamma^n(u_L, u_R, \bar{x}, T)$

crosses. One of them is chosen randomly using the Matlab function rand.

In Figure 9 and Figure 10, six different initial data u_0^n are constructed generating weak-entropy solutions that coincide with the target $u^T(\cdot) = 0.6875\mathbb{1}_{(-\infty,4.6)}(\cdot) - \mathbb{1}_{(4.6,\infty)}(\cdot)$ at time $T = 1$. The discretization parameter is $n = 4$, the state mesh is $\mathcal{M}_n := -1 + 3(2^{-n}\mathbb{N} \cap [0,1])$ and M stands for the number of discontinuous points of u_0^n. Note that the backward maximum principle is violated in the case $M = 2$, $M = 3$, $M = 5$ and $M = 6$. Since $\mathcal{M}_n := -1 + 3(2^{-n}\mathbb{N} \cap [0,1])$, the initial data u_0^n constructed verifies $-1 \leq u_0^n \leq 2$. If our aim is to construct admissible initial data u_0^n such that $M_1 \leq u_0^n \leq M_2$ with $M_1 < -1$ and $2 < M_2$, either we modify the state mesh $\mathcal{M}_n$ by $\mathcal{M}_n := M_1 + (M_2 - M_1)(2^{-n}\mathbb{N} \cap [0,1])$ or we use that $\{u_0 \in BV(\mathbb{R})/S_T^+(u_0) = u^T\}$ is a convex cone having as unique extremal point at its vertex the map $S_T^-(u^T)$ as follows. For every $\eta > 0$, the initial data $u_0^{\eta,n} := S_T^{-,n}(u^T) + \eta(u_0^n - S_T^{-,n}(u^T))$ with u_0^n constructed in Figure 10 also leads to u^T at time $T = 1$ and we notice that $\lim_{\eta\to\infty} \|u_0^{\eta,n}\|_\infty = +\infty$.

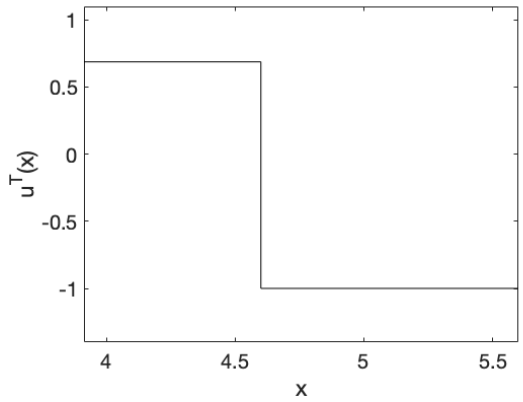

Figure 9: The target u^T defined by $u^T(\cdot) = 0.6875\mathbb{1}_{(-\infty,4.6)}(\cdot) - \mathbb{1}_{(4.6,\infty)}(\cdot)$

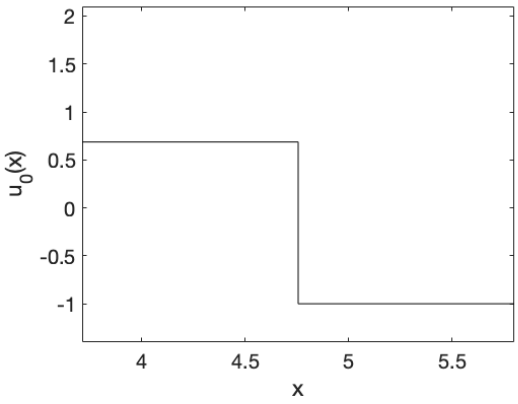

$M = 1$ discontinuous point

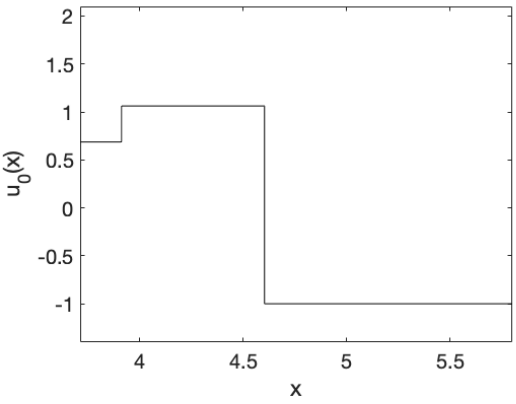

$M = 2$ discontinuous points

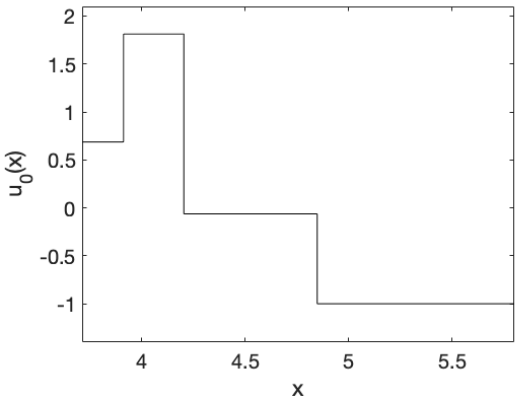

$M = 3$ discontinuous points

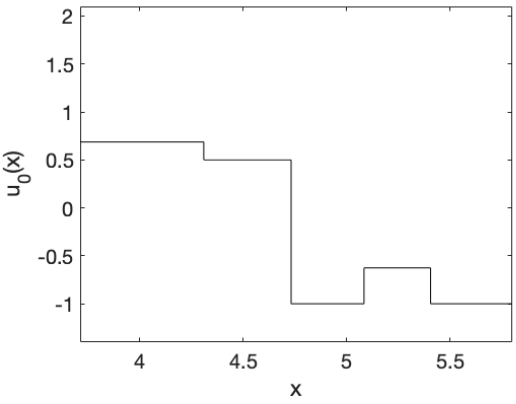

$M = 4$ discontinuous points

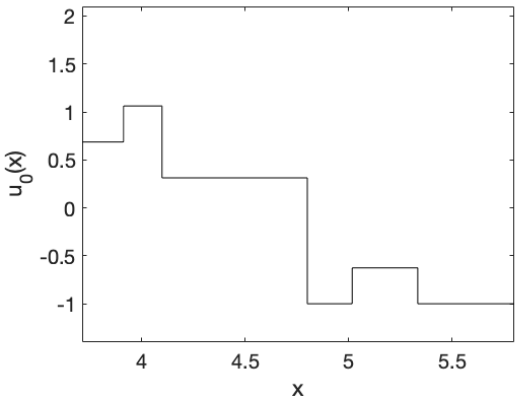

$M = 5$ discontinuous points

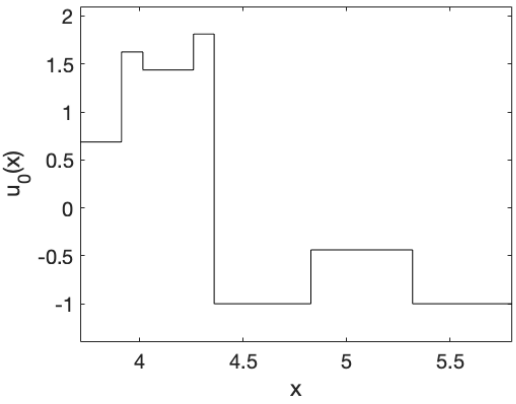

$M = 6$ discontinuous points

Figure 10: Construction of six random initial data u_0^n such that u_0^n admits $M \in \{1, \cdots, 6\}$ discontinuous points, $S_T^{+,n}(u_0^n) = u^T$ with $u_L = 0.6875$, $u_R = -1$, $T = 1$, $\bar{x} = 4.6$ and $n = 4$

3.4 Construction of the set of minimizers of $(\mathcal{O}_T)$

In this section, we describe the algorithm used to solve the optimal problem $(\mathcal{O}_T)$.

Algorithm. Algorithm for the construction of the set of optimal solutions for $(\mathcal{O}_T)$

Input data:

- The target function u^T
- The discontinuous points of u^T denoted by $(x_i^T)_{i=1,\cdots,N}$ with $N \in \mathbb{N}$.
- For every $i \in \{1, \cdots, N\}$, the values $u^T(x_i^T-)$ and $u^T(x_i^T+)$.

Step 0. Construction of a state mesh $\mathcal{M}_n$ and an approximate target $u^{T,n} : \mathbb{R} \to \mathcal{M}_n$ of u^T as described in Section 3.1.

Step 1.

- Construction of an approximate function $S_T^{-,n}(u^{T,n})$ of $S_T^-(u^T)$ using the wave-front tracking algorithm described in Section 3.1.
- Construction of an approximate function $S_T^{+,n}(S_T^{-,n}(u^{T,n}))$ of $S_T^+(S_T^-(u^T))$ using the wave-front tracking algorithm described in Section 3.1.

Step 2. Construction of all initial data u_0^n such that $S_T^{+,n}(u_0^n) = S_T^{+,n}(S_T^{-,n}(u^{T,n}))$ using Section 3.3.

- We find the set of discontinuous points $(x_j^{*,n})_{i=1,\cdots,N_n^*}$ of $S_T^{+,n}(S_T^{-,n}(u^{T,n}))$ such that for every $i \in \{1, \cdots, N_n^*\}$, $S_T^{+,n}(S_T^{-,n}(u^{T,n}))(x_j^{*,n}-) > S_T^{+,n}(S_T^{-,n}(u^{T,n}))(x_j^{*,n}+)$. To simplify the notations,
$$u_L^j := S_T^{+,n}(S_T^{-,n}(u^{T,n}))(x_j^{*,n}-),$$
and
$$u_R^j := S_T^{+,n}(S_T^{-,n}(u^{T,n}))(x_j^{*,n}+).$$
- At each point $x_j^{*,n}$, we construct a random initial datum $u_j^{*,n}$ such that
$$S_T^{+,n}(u_j^{*,n}) = u_L^j \mathbb{1}_{(-\infty, x_j^{*,n})} + u_R^j \mathbb{1}_{(x_j^{*,n}, \infty)},$$
using Section 3.3. More precisely, we construct $\gamma_j^n \in \Gamma(u_L^j, u_R^j, x_j^{*,n}, T)$ such that
$$u_0^n(x) = \begin{cases} u_L^j, & \text{for every } x < x_j^{*,n} - Tf'(u_L^j), \\ \dot{\gamma}_j^n(x), & \text{for a.e } x \in [x_j^{*,n} - Tf'(u_L^j), x_j^{*,n} - Tf'(u_R^j)], \\ u_R^j, & \text{for every } x_j^{*,n} - Tf'(u_R^j) < x. \end{cases}$$
- We construct a random optimal solution $u_0^{\text{rand},n}$ of $(\mathcal{O}_T)$ piecing together every $u_j^{*,n}$ with $S_T^{-,n}(u^{T,n})$ as described in Section 3.3. More precisely, we have, for a.e $x \in \mathbb{R}$,
$$u_0^{\text{rand},n}(x) = \begin{cases} u_j^{*,n}(x) & \text{if } x \in [x_j^{*,n} - Tf'(u_L^j), x_j^{*,n} - Tf'(u_R^j)],\ j \in \{1, \cdots, N_n^*\}, \\ S_T^{-,n}(u^{T,n})(x) & \text{otherwise.} \end{cases}$$

Output data:

- The approximate backward entropy solution $S_T^{-,n}(u^{T,n})$,
- A random approximate optimal solution $u_0^{\text{rand},n}$.

We give the two following examples to illustrate the algorithm described above.

Example 4 *Let $T = 2$. We consider the target u^T defined as*

$$u^T(x) = \begin{cases} 2 & \text{if } x \in (-0.2, 1.1) \bigcup (2, 3.1) \bigcup (4.1, 5.3) \bigcup (6.1, 7.2), \\ -1 & \text{otherwise.} \end{cases}$$

Since for every $x \in \{-0.2, 2, 4.1, 6.1\}$, we have $u^T(x-) + 3 = u^T(x+)$, u^T is an unattainable target. From Theorem 2.1, $S_T^+(S_T^-(u^T))$ is an optimal solution of $(\mathcal{O}_T)$. Firstly, we construct an approximate function $S_T^{+,n}(S_T^{-,n}(u^T))$ of $S_T^+(S_T^-(u^T))$ using the wave-front tracking algorithm described in Section 3.1. The discretization parameter is $n = 8$ and the state mesh $\mathcal{M}_n$ is defined by $\mathcal{M}_n = -1 + 3(2^{-n}\mathbb{N} \cap [0, 1])$. In this example, we have $u^{T,n} = u^T$.

- *In Figure 11a), the function $(t, x) \to S_t^{-,n}(u^T)(-x)$ is plotted.*
- *In Figure 11b), the approximate optimal solution $S_T^{-,n}(u^T)$ of $(\mathcal{O}_T)$ is plotted.*
- *In Figure 11c), the function $(t, x) \to S_t^{+,n}(S_T^{-,n}(u^T))(x)$ is plotted.*
- *In Figure 11d), the function u^T and $x \to S_T^{+,n}(S_T^{-,n}(u^T))(x)$ are plotted.*

*Secondly, we give four different $u_0^{rand,n}$ such that $S_T^{+,n}(u_0^{rand,n}) = S_T^{+,n}(S_T^{-,n}(u^T))$ illustrating the **Step 2.** of the algorithm above, see Figure 12.*

Example 5 *Let $T = 1$. We consider the target u^T defined as*

$$\begin{aligned} u^T = \quad & -1\!\!1_{(-\infty,0)} + 3\!1\!\!1_{(0,1.1)} + 0.55\!1\!\!1_{(1.1,2)} + 2.11\!1\!\!1_{(2,3.1)} - 0.7\!1\!\!1_{(3.1,5)} \\ & -0.23\!1\!\!1_{(5,5.8)} - 1\!\!1_{(5.8,6.1)} + 2.89\!1\!\!1_{(6.1,7.2)} - 1\!\!1_{(7,2,\infty)}. \end{aligned}$$

The function u^T is an unattainable target. The discretization parameter $n = 8$ and the state mesh $\mathcal{M}_n$ is defined by $\mathcal{M}_n = -1 + 4(2^{-n}\mathbb{N} \cap [0, 1])$. In Figure 13, the function u^T and $x \to S_T^{+,n}(S_T^{-,n}(u^T))(x)$ are plotted.

4 Proof of Theorem 2.1

Using the forward maximum principle and the finite velocity of propagation that entropy solutions fulfilled, we immediately deduce that

Lemma 4.1 *We assume that $supp(u^T) \subset K^T$ with K^T defined in Section 2.2 and $u_0 \in \mathcal{U}_{ad}^0$. Then, $supp(S_T^-(u^T))$ is an open bounded interval and there exists an open bounded interval $\tilde{K} \subset \mathbb{R}$ such that, for every $u_0 \in \mathcal{U}_{ad}^0$, $Supp(S_T^+(u_0)) \subset \tilde{K}$.*

The proof of Theorem 2.1 is based on the following Lemma.

Lemma 4.2 *For every open bounded interval $K_1 \subset \mathbb{R}$ such that $\tilde{K} \subset K_1$ and for every $C > 0$ such that $\|u^T\|_{BV(\mathbb{R})} < C$, the optimal problem (4) admits a unique minimizer q^* defined by, for a.e $x \in \mathbb{R}$,*

$$q^*(x) = S_T^+(S_T^-(u^T))(x).$$

Above, $\tilde{K}$ is defined in Lemma 4.1.

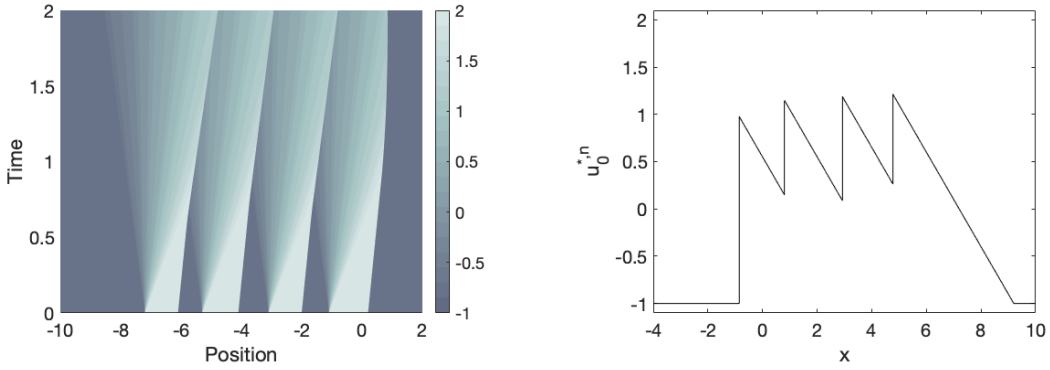

a) $(t,x) \to S_t^{-,n}(u^T)(-x)$ **b)** $x \to S_T^{-,n}(u^T)(x)$

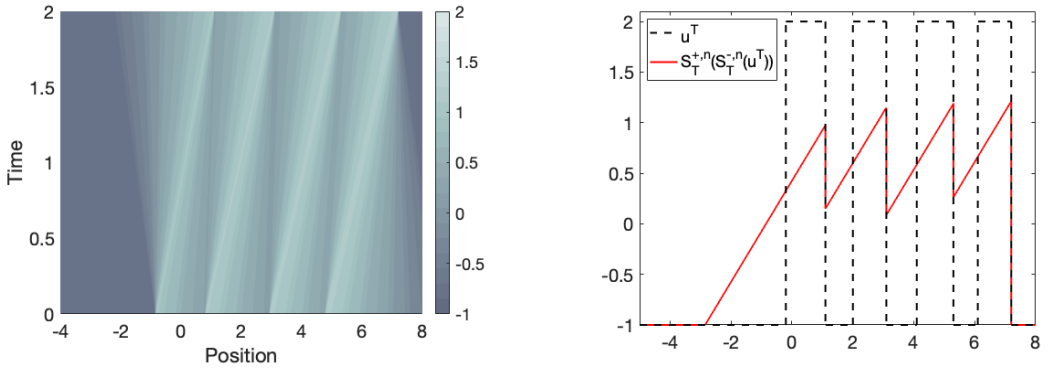

c) $(t,x) \to S_t^{+,n}(S_T^{-,n}(u^T))(x)$ **d)** u^T and $x \to S_T^{+,n}(S_T^{-,n}(u^T))(x)$

Figure 11: $T = 2$, $n = 8$. Illustration of the **Algorithm Step 1** described in Section 3.4 where the unattainable target u^T is defined in Example 4.

Proof. The proof is divided in two steps.

Step 1: Existence and uniqueness of minimizers of (4)**.** By definition of J_1, it is enough to prove that $\mathcal{U}_{\text{ad}}^T$ is a closed convex set of $L^2(\mathbb{R})$ using Hilbert projection Theorem. Assuming that $q_1, q_2 \in \mathcal{U}_{\text{ad}}^T$ we immediately have, for every $\alpha \in [0,1]$, $\alpha q_1 + (1-\alpha)q_2 \in \mathcal{U}_{\text{ad}}^1$. Moreover, if q_n converges to q in $L^2(\mathbb{R})$ then q_n converges to q in the sense of distributions and by passing to the limit in $\partial_x q_n \leq \frac{1}{T}$, we have $\partial_x q \leq \frac{1}{T}$. Using that $\|q_n\|_{BV(\mathbb{R})} \leq C$ and $\text{Supp}(q_n) \subset K_1$, from Helly's compactness theorem, we have

$$\lim_{n\to\infty} q_n = q \text{ in } L^1(K_1) \text{ and } TV_{K_1}(q) \leq \liminf_n TV_{K_1}(q_n). \tag{7}$$

From (7), we deduce that $q \in BV(K_1)$. Since q_n converges to q in $L^2(\mathbb{R})$, q_n converges a.e to q. Moreover, for a.e $x \in \mathbb{R}\backslash K_1$, $q_n(x) = 0$. Thus,

$$\text{Supp}(q) \subset K_1. \tag{8}$$

From (7) and (8), we conclude that $\|q\|_{BV(\mathbb{R})} \leq \liminf_n \|q_n\|_{BV(\mathbb{R})} \leq C$ and thus $q \in \mathcal{U}_{\text{ad}}^T$. Since J_1 is a strictly convex function, there exists a unique minimizer q^* of (4). Note that q^* is the

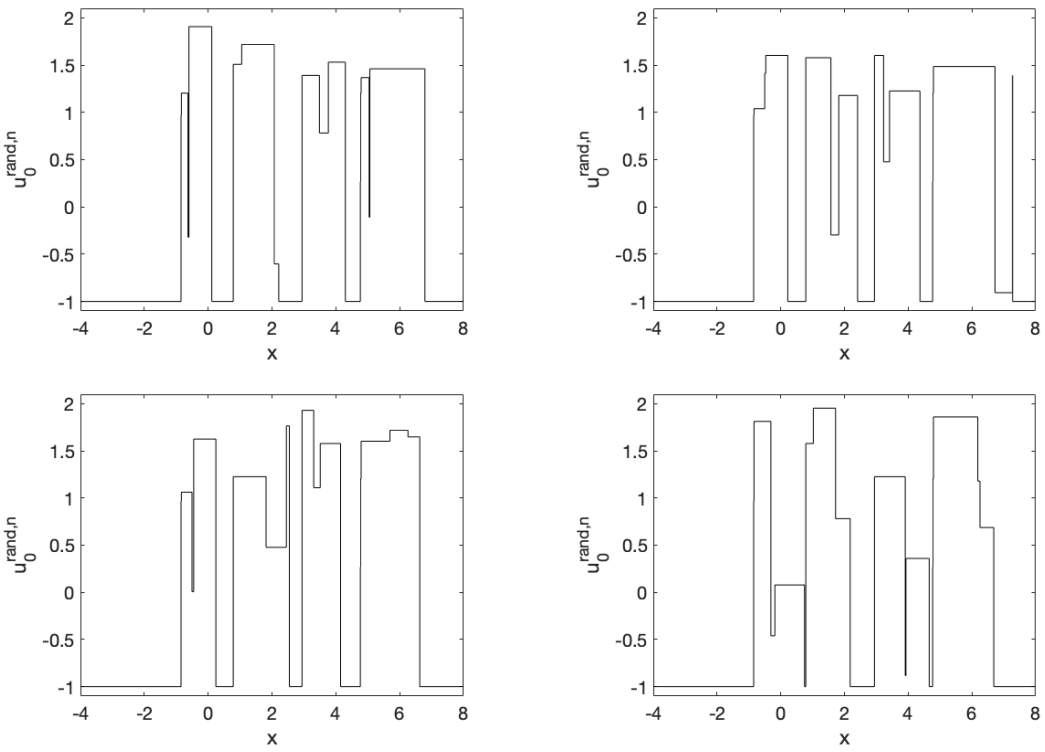

Figure 12: $T = 2$, $n = 8$. Four different $u_0^{\text{rand},n}$ such that $S_T^{+,n}(u_0^{\text{rand},n}) = S_T^{+,n}(S_T^{-,n}(u^T))$ with u^T defined in Example 4.

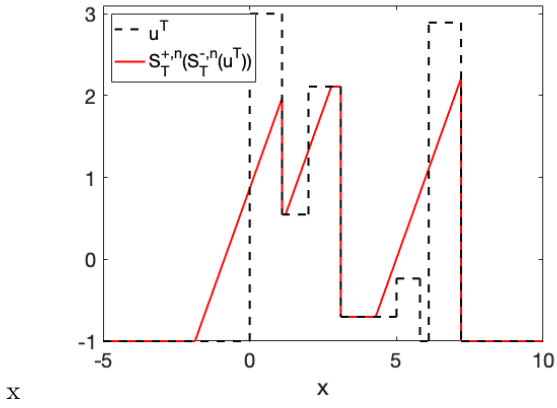

Figure 13: u^T and $x \to S_T^{+,n}(S_T^{-,n}(u^T))(x)$ with u^T defined in Example 5

projection of u^T onto $\mathcal{U}_{\text{ad}}^1$.

Step 2: First-order optimality conditions. Our aim is to prove that, for any admissible

perturbation $h \in \mathcal{T}_{S_T^+(S_T^-(u^T))}$[1], we have

$$-\int_{\mathbb{R}} \left(u^T(x) - S_T^+(S_T^-(u^T))(x)\right) h(x)\,dx \geq 0. \tag{9}$$

By definition of S_T^- and S_T^+ (see Section 2.1) and [20, Theorem 11.3.5], for a.e $T > 0$, we have $S_T^-(S_T^+(S_T^-(u^T)) = S_T^-(u^T) \in SBV(\mathbb{R})$. Therefore, there exist at most countable number of points $(x_0^i)_{i\in\{0,\cdots N\}}$ such that $S_T^-(u^T)(x_0^i-) < S_T^-(u^T)(x_0^i+)$ with $N \in \mathbb{N} \cup \{+\infty\}$. Applying Theorem A.2 with $u_0 = S_T^-(u^T)$, we have

- For every $x \in \mathbb{R}\setminus \cup_{i=1}^N [\underline{b}_i, \overline{b}_i]$,

$$u^T(x-) = S_T^+(S_T^-(u^T))(x-). \tag{10}$$

- For every $x \in \cup_{i=1}^N [\underline{b}_i, \overline{b}_i]$

$$\int_{\underline{b}_i}^x u^T(s)\,ds \leq \int_{\underline{b}_i}^x S_T^+(S_T^-(u^T))(s)\,ds, \tag{11}$$

$$\int_{\underline{b}_i}^{\overline{b}_i} u^T(s)\,ds = \int_{\underline{b}_i}^{\overline{b}_i} S_T^+(S_T^-(u^T))(s)\,ds, \tag{12}$$

with $\underline{b}_i := x_0^i + Tf'(S_T^-(u^T)(x_0^i-))$ and $\overline{b}_i := x_0^i + Tf'(S_T^-(u^T)(x_0^i+))$. We denote by $\xi_{\bar{x}}(t)$ the forward characteristic, associated with $S_t^+(S_T^-(u^T))$, emanating from $(0,\bar{x})$. By construction of S_t^-, for every $\bar{x}, \bar{y} \in \mathbb{R}\setminus \cup_{i=1}^N \{x_0^i\}$, $\xi_{\bar{x}}(\cdot)$ doesn't interact with $\xi_{\bar{y}}(\cdot)$ over $(0,T)$. In particular, for every $\bar{x} \in \mathbb{R}\setminus \cup_{i=1}^N \{x_0^i\}$, for every $t \in [0,T]$,

$$\xi_{\bar{x}}(t) \notin \cup_{i=1}^n (x_0^i + tf'(S_T^-(u^T)(x_0^i-)), x_0^i + tf'(S_T^-(u^T)(x_0^i+))). \tag{13}$$

Since $S_T^-(u^T)(x_0^i-) < S_T^-(u^T)(x_0^i+)$, a rarefaction wave is created at $(0, x_0^i)$. From (13), we deduce that for every $x \in (x_0^i + Tf'(S_T^-(u^T)(x_0^i-)), x_0^i + Tf'(S_T^-(u^T)(x_0^i+)))$,

$$\partial_x S_T^+(S_T^-(u^T))(x) = \frac{1}{T}. \tag{14}$$

We have

$$\begin{aligned} -\textstyle\int_{\mathbb{R}}(u^T(x) - S_T^+(S_T^-(u^T))(x))h(x)\,dx = \quad & -\textstyle\int_{\mathbb{R}\setminus\cup_{i=1}^N(\underline{b}_i,\overline{b}_i)}(u^T(x) - S_T^+(S_T^-(u^T)))h(x)\,dx \\ & -\textstyle\sum_{i=1}^N \int_{\underline{b}_i}^{\overline{b}_i}(u^T(x) - S_T^+(S_T^-(u^T)))h(x)\,dx. \end{aligned} \tag{15}$$

From (10), for every $h \in \mathcal{T}_{S_T^+(S_T^-(u^T))}$,

$$\int_{\mathbb{R}\setminus\cup_{i=1}^N(\underline{b}_i,\overline{b}_i)} (u^T(x) - S_T^+(S_T^-(u^T)))h(x)\,dx = 0. \tag{16}$$

[1]That is a set of functions $h \in L^2(\mathbb{R})$ such that, for any sequence of positive real numbers ϵ_n decreasing to 0, there exists a sequence of functions $h_n \in L^2(\mathbb{R})$ converging to h as $n \to \infty$ and $S_T^+(S_T^-(u^T)) + \epsilon_n h_n \in \mathcal{U}_{\text{ad}}^1$ for every $n \in \mathbb{N}$.

To prove that, for every $i \in \{1, \cdots, \mathbb{N}\}$ and for any admissible perturbation $h \in \mathcal{T}_{S_T^+(S_T^-(u^T)}$, $-\int_{\underline{b}_i}^{\bar{b}_i}(u^T(x) - S_T^+(S_T^-(u^T))(x))h(x)\,dx \geq 0$, we introduce the function F defined by, for every $x \in [\underline{b}_i, \bar{b}_i]$,

$$F(x) = \int_{\underline{b}_i}^{x} \left(u^T(s) - S_T^+(S_T^-(u^T))(s)\right)\,ds. \tag{17}$$

From (11) and (12), $F \in W_0^{1,2}(\underline{b}_i, \bar{b}_i)$ and $F \leq 0$. Since $h \in \mathcal{T}_{S_T^+(S_T^-(u^T))}$ is an admissible perturbation then for every $\epsilon_n > 0$ such that $\epsilon_n \to 0$ when $n \to \infty$ there exists $h_n \in L^2(\mathbb{R})$ such that $\lim_{n\to\infty} h_n = h$ in $L^2(\mathbb{R})$ and $S_T^+(S_T^-(u^T)) + \epsilon_n h_n \in \mathcal{U}_{\rm ad}^T$. Thus, from (14), $\partial_x h_n \leq 0$. Since $\lim_{n\to\infty} h_n = h$ in $L^2(\mathbb{R})$, h_n tends to h in the sense of distributions and we conclude that for any admissible perturbation $h \in \mathcal{T}_{q^*}$

$$\partial_x h \leq 0. \tag{18}$$

Using a mollifier function ρ_n, there exists $F_n := \rho_n * F \in C_c^\infty(\underline{b}_i, \bar{b}_i)$ such that F_n converges to F in $W_0^{1,2}(\underline{b}_i, \bar{b}_i)$. Moreover, since $F \leq 0$, we also have $F_n \leq 0$. From (18), for every $n \in \mathbb{N}$

$$-\int_{\underline{b}_i}^{\bar{b}_i} F_n'(x)h(x)\,dx = \left\langle F_n, \partial_x h\right\rangle \geq 0. \tag{19}$$

Since F_n converges to F in $W_0^{1,2}(\underline{b}_i, \bar{b}_i)$, F_n' converges to F' in $L^2(\underline{b}_i, \bar{b}_i)$. Therefore, by passing to the limit in (19), we conclude that, for any admissible perturbation $h \in \mathcal{T}_{S_T^+(S_T^-(u^T)}$,

$$-\int_{\underline{b}_i}^{\bar{b}_i} (u^T(x) - S_T^+(S_T^-(u^T))(x))h(x)\,dx \geq 0. \tag{20}$$

From (15), (16) and (20), the inequality (9) holds. Thus, $S_T^+(S_T^-(u^T))$ is a critical point of (4). Since J_1 is strictly convex, $S_T^+(S_T^-(u^T))$ is the unique optimal solution of (4).

□

Proof of Theorem 2.1: From Lemma 4.2, for every $q \in \mathcal{U}_{\rm ad}^T$, we have

$$\|u^T - S_T^+(S_T^-(u^T))\|_{L^2(\mathbb{R})} \leq \|u^T - q\|_{L^2(\mathbb{R})}. \tag{21}$$

Since $\mathrm{Supp}(S_T^-(u^T)) \subset K_0$, $\|S_T^-(u^T)\|_{BV(\mathbb{R})} \leq C$, we have $S_T^-(u^T) \in \mathcal{U}_{\rm ad}^0$. Moreover, for every $u_0 \in \mathcal{U}_{\rm ad}^0$, $S_T^+(u_0) \in \mathcal{U}_{\rm ad}^T$ since

- $\mathrm{Supp}(S_T^+(u_0)) \subset \tilde{K} \subset K_1$ with $\tilde{K}$ defined in Lemma 4.1.
- From [20, 11.2.2 Theorem] and $\mathrm{Supp}(S_T^+(u_0)) \subset K_1$, we have $S_T^+(u_0) \in BV(\mathbb{R})$ and $\partial_x S_T^+(u_0) \leq \frac{1}{T}$.
- From [20, 6.2.3 Theorem, 6.2.6 Theorem] and $\mathrm{Supp}(S_T^+(u_0)) \subset K_1$, we have $\|S_T^+(u_0)\|_{BV(\mathbb{R})} \leq \|u_0\|_{BV(\mathbb{R})} \leq C$.

From (21) and for every $u_0 \in \mathcal{U}_{\rm ad}^0$, $S_T^+(u_0) \in \mathcal{U}_{\rm ad}^T$, we conclude that, for every $u_0 \in \mathcal{U}_{\rm ad}^0$,

$$\|u^T - S_T^+(S_T^-(u^T))\|_{L^2(\mathbb{R})} \leq \|u^T - S_T^+(u_0)\|_{L^2(\mathbb{R})}, \tag{22}$$

which concludes the proof of Theorem 2.1.

A Characterization of the set of initial data evolving to the same target u^T at time T

Theorem A.1 gives a full characterization of the set of initial data $u_0 \in BV(\mathbb{R})$ such that $S_T^+(u_0) = u^T$.

Theorem A.1 *Assuming that $u^T \in SBV(\mathbb{R})$ and $\partial_x u^T \leq \frac{1}{T}$. We denote by $(x_i^T)_{i\in\{0,\cdots,N\}}$ the $N \in \mathbb{N}\cup\{\infty\}$ discontinuous points of u^T such that $u^T(x_i^T+) < u^T(x_i^T-)$ and $\underline{a}_i := x_i^T - Tf'(u^T(x_i^T-))$ and $\overline{a}_i := x_i^T - Tf'(u^T(x_i^T+))$. A map $u_0 \in BV(\mathbb{R})$ verifies $S_T^+(u_0) = u^T$ if and only if the two following statements hold:*

- *For every $x \in \mathbb{R}\setminus \cup_{i=1}^N [\underline{a}_i, \overline{a}_i]$, $u_0(x-) = S_T^-(u^T)(x-)$.*
- *For every $x \in \cup_{i=1}^N [\underline{a}_i, \overline{a}_i]$,*

$$\int_{\underline{a}_i}^{x} u_0(s)\,ds \geq \int_{\underline{a}_i}^{x} S_T^-(u^T)(s)\,ds,$$
$$\int_{\underline{a}_i}^{\overline{a}_i} u_0(s)\,ds = \int_{\underline{a}_i}^{\overline{a}_i} S_T^-(u^T)(s)\,ds.$$

The proof is given in [15, Theorem 4.1]. Theorem A.2 gives a full characterization of the set of function $u^T \in SBV(\mathbb{R})$ such that $S_T^-(u^T) = u_0$.

Theorem A.2 *Assuming that $u_0 \in SBV(\mathbb{R})$ and $\partial_x u_0 \geq -\frac{1}{T}$. We denote by $(x_0^i)_{i\in\{0,\cdots,N\}}$ the $N \in \mathbb{N}\cup\{\infty\}$ discontinuous points of u_0 such that $u_0(x_0^i-) < u_0(x_0^i+)$ and $\underline{b}_i := x_0^i + Tf'(u_0(x_0^i-))$ and $\overline{b}_i := x_0^i + Tf'(u_0(x_0^i+))$. A map $u^T \in BV(\mathbb{R})$ verifies $S_T^-(u^T) = u_0$ if and only if the two following statements hold:*

- *For every $x \in \mathbb{R}\setminus \cup_{i=1}^N [\underline{b}_i, \overline{b}_i]$,*
$$u^T(x-) = S_T^+(u_0)(x-). \tag{23}$$
- *For every $x \in \cup_{i=1}^N [\underline{b}_i, \overline{b}_i]$,*

$$\int_{\underline{b}_i}^{x} u^T(s)\,ds \leq \int_{\underline{b}_i}^{x} S_T^+(u_0)(s)\,ds,$$
$$\int_{\underline{b}_i}^{\overline{b}_i} u^T(s)\,ds = \int_{\underline{b}_i}^{\overline{b}_i} S_T^+(u_0)(s)\,ds. \tag{24}$$

Theorem A.2 is a consequence of Theorem A.1 noticing that $S_T^-(u^T) : x \to S_T^+(x \to u^T(-x))(x)$.

References

[1] Navid Allahverdi, Alejandro Pozo, and Enrique Zuazua. Numerical aspects of large-time optimal control of burgers equation. *ESAIM: Mathematical Modelling and Numerical Analysis*, 50(5):1371–1401, 2016.

[2] Navid Allahverdi, Alejandro Pozo, and Enrique Zuazua. Numerical aspects of sonic-boom minimization. *A Panorama of Mathematics: Pure and Applied*, 658:267, 2016.

[3] Juan J Alonso and Michael R Colonno. Multidisciplinary optimization with applications to sonic-boom minimization. *Annual Review of Fluid Mechanics*, 44:505–526, 2012.

[4] Claude Bardos, Olivier Pironneau, et al. Data assimilation for conservation laws. *Methods and Applications of Analysis*, 12(2):103–134, 2005.

[5] Andrew F Bennett. *Inverse modeling of the ocean and atmosphere*. Cambridge University Press, 2005.

[6] François Bouchut and François James. One-dimensional transport equations with discontinuous coefficients. *Nonlinear Analysis*, 32(7):891, 1998.

[7] François Bouchut and François James. Differentiability with respect to initial data for a scalar conservation law. In *Hyperbolic problems: theory, numerics, applications*, pages 113–118. Springer, 1999.

[8] Alberto Bressan and Rinaldo M Colombo. Decay of positive waves in nonlinear systems of conservation laws. *Annali della Scuola Normale Superiore di Pisa-Classe di Scienze*, 26(1):133–160, 1998.

[9] Alberto Bressan and Andrea Marson. A maximum principle for optimally controlled systems of conservation laws. *Rendiconti del Seminario Matematico della Universita di Padova*, 94:79–94, 1995.

[10] Alberto Bressan and Andrea Marson. A variational calculus for discontinuous solutions of systems of conservation laws. *Communications in partial differential equations*, 20(9):1491–1552, 1995.

[11] Carlos Castro, Francisco Palacios, and Enrique Zuazua. An alternating descent method for the optimal control of the inviscid burgers equation in the presence of shocks. *Mathematical Models and Methods in Applied Sciences*, 18(03):369–416, 2008.

[12] Carlos Castro, Francisco Palacios, and Enrique Zuazua. Optimal control and vanishing viscosity for the burgers equation. In *Integral Methods in Science and Engineering, Volume 2*, pages 65–90. Springer, 2010.

[13] Christophe Chalons. Transport-equilibrium schemes for pedestrian flows with nonclassical shocks. In *Traffic and Granular Flow'05*, pages 347–356. Springer, 2007.

[14] Robin Olav Cleveland. *Propagation of sonic booms through a real, stratified atmosphere*. PhD thesis, Citeseer, 1995.

[15] Rinaldo Colombo and Vincent Perrollaz. Initial data identification in conservation laws and hamilton-jacobi equations. *arXiv preprint arXiv:1903.06448*, 2019.

[16] Rinaldo M Colombo and Massimiliano D Rosini. Pedestrian flows and non-classical shocks. *Mathematical methods in the applied sciences*, 28(13):1553–1567, 2005.

[17] Michael G Crandall and Andrew Majda. Monotone difference approximations for scalar conservation laws. *Mathematics of Computation*, 34(149):1–21, 1980.

[18] Dacian N Daescu and Ionel Michael Navon. Adaptive observations in the context of 4d-var data assimilation. *Meteorology and Atmospheric Physics*, 85(4):205–226, 2004.

[19] Constantine M Dafermos. Polygonal approximations of solutions of the initial value problem for a conservation law. *Journal of Mathematical Analysis and Applications*, 38(1):33–41, 1972.

[20] Constantine M Dafermos. Hyperbolic conservation laws in continuum physics, volume 325 of grundlehren der mathematischen wissenschaften [fundamental principles of mathematical sciences], 2010.

[21] Michael Ghil and Paola Malanotte-Rizzoli. Data assimilation in meteorology and oceanography. In *Advances in geophysics*, volume 33, pages 141–266. Elsevier, 1991.

[22] Shyam Sundar Ghoshal, GD Veerappa Gowda, et al. Exact controllability of scalar conservation laws with strict convex flux. *Mathematical Control & Related Fields*, 4(4):401, 2014.

[23] Olivier Glass. An extension of oleinik's inequality for general 1d scalar conservation laws. *Journal of Hyperbolic Differential Equations*, 5(1):113, 2008.

[24] Laurent Gosse and Enrique Zuazua. Filtered gradient algorithms for inverse design problems of one-dimensional burgers equation. In *Innovative algorithms and analysis*, pages 197–227. Springer, 2017.

[25] Helge Holden and Nils Henrik Risebro. A method of fractional steps for scalar conservation laws without the cfl condition. *Mathematics of computation*, 60(201):221–232, 1993.

[26] Eugenia Kalnay. *Atmospheric modeling, data assimilation and predictability*. Cambridge university press, 2003.

[27] Stanislav N Kružkov. First order quasilinear equations in several independent variables. *Mathematics of the USSR-Sbornik*, 10(2):217, 1970.

[28] Peter D Lax. Hyperbolic systems of conservation laws ii. *Communications on pure and applied mathematics*, 10(4):537–566, 1957.

[29] François-Xavier Le Dimet and Olivier Talagrand. Variational algorithms for analysis and assimilation of meteorological observations: theoretical aspects. *Tellus A: Dynamic Meteorology and Oceanography*, 38(2):97–110, 1986.

[30] Randall J LeVeque and Randall J Leveque. *Numerical methods for conservation laws*, volume 132. Springer, 1992.

[31] Yingying Li, Stanley Osher, and Richard Tsai. Heat source identification based onconstrained minimization. *Inverse Problems and Imaging*, 8(1):199–221, 2014.

[32] J-L Lions and Bernard Malgrange. Sur l'unicité rétrograde dans les problèmes mixtes paraboliques. *Mathematica Scandinavica*, 8(2):277–286, 1961.

[33] Andrew Majda. *The existence of multi-dimensional shock fronts*, volume 281. American Mathematical Soc., 1983.

[34] Andrew Majda. *The stability of multi-dimensional shock fronts*, volume 275. American Mathematical Soc., 1983.

[35] Olga Arsen'evna Oleinik. Discontinuous solutions of non-linear differential equations. *Uspekhi Matematicheskikh Nauk*, 12(3):3–73, 1957.

[36] Yannick Privat, Emmanuel Trélat, and Enrique Zuazua. Optimal location of controllers for the one-dimensional wave equation. *Ann. Inst. H. Poincaré Anal. Non Linéaire*, 30(6):1097–1126, 2013.

[37] Yannick Privat, Emmanuel Trélat, and Enrique Zuazua. Optimal observation of the one-dimensional wave equation. *J. Fourier Anal. Appl.*, 19(3):514–544, 2013.

[38] Yannick Privat, Emmanuel Trélat, and Enrique Zuazua. Optimal shape and location of sensors for parabolic equations with random initial data. *Archive for Rational Mechanics and Analysis*, 216(3):921–981, 2014.

[39] Kyle Swanson, Robert Vautard, and Carlos Pires. Four-dimensional variational assimilation and predictability in a quasi-geostrophic model. *Tellus A: Dynamic Meteorology and Oceanography*, 50(4):369–390, 1998.

[40] Olivier Talagrand and Philippe Courtier. Variational assimilation of meteorological observations with the adjoint vorticity equation. i: Theory. *Quarterly Journal of the Royal Meteorological Society*, 113(478):1311–1328, 1987.